

UDC 53.03; 51-71

NUMERICAL MODEL OF MOTION OF ELECTRON IN GAS

D.V. Kiryushin, D.E. Korytchinkov, D.V. Suvorov, A.A. Trubitsyn, V.N. Shurikov

Ryazan State Radio Engineering University, 390005, Gagarin st., 59/1, assur@bk.ru

Numerical model of electron movement inside gas media was developed. Respective software module integrated into author's software application designed for numerical investigation of electron optic systems was obtained. Experimental test of the developed model was performed and discussed.

Keywords: gas media, electron optic systems, electron movement, numerical model, numerical investigation.

Introduction

Plasma of electric discharges in gas is neutral on a whole, since concentrations of positive and negative particles are equal. However due to the fact that the electron mobility is at least 1000 times higher than the positive ion mobility, discharge current is mostly the electron current with just a small portion of ion current.

It means that a study of nature and influences of various external factors - e.g. magnetic fields effects - on three-dimensional configuration of a discharge must necessarily involve a study of electrons' passage since the electrons are just the prime source of discharge generation when colliding with gas molecules.

Often enough there appears a need to study the effects of residual gas on the electron-optical systems. A task of this kind can be solved by means of simulating paths of a plurality of electrons colliding with gas molecules.

Numerical computing methods designed to determine the macro parameters of certain process using some known parameters are based on the Monte Carlo method which basically means simulation of said macro parameters and involves a large number of statistic tests to be conducted

1. Simulation of an electron free path length

On a first approximation the length of an electron free path - which is understood an average distance covered by an electron between two successive collisions with gas molecules - can be obtained by means of the following formula [1]

$$\lambda_0 = \frac{4kT}{\pi P d^2}, \quad (1)$$

where P is the gas pressure, k is the Boltzmann's constant, T is the gas temperature and d is the molecule diameter.

More precise collision models need to incorporate relation between free path length and energy E. Presented in Fig. 1a are relations between probability of electron collisions with gas molecules and electron energy of various gases obtained by means of quantum-mechanical calculations [2]. Analysis of graphs shows that the collision probability - in particular, for N₂-molecules - within energy range from some fractions of eV to 2 eV is approximately three-times increased with a further trend to monotonic decrease, in particular within a range from 2 to 10 eV the collision probability is approximately five-times decreased.

Since free-path length and collision probability are inversely proportional quantities, under consideration of a.m. factors relation between the electron free-path length and electron energy when colliding with N₂-molecules can be approximated by means of the following function (refer to Fig. 1b)

$$\lambda_E = \lambda_0 \cdot g(E), \quad (2)$$

$$\text{where } g(E) = \begin{cases} 3 - E, & 0 \leq E < 2, \\ 1 + \ln(E - 1), & E \geq 2. \end{cases}$$

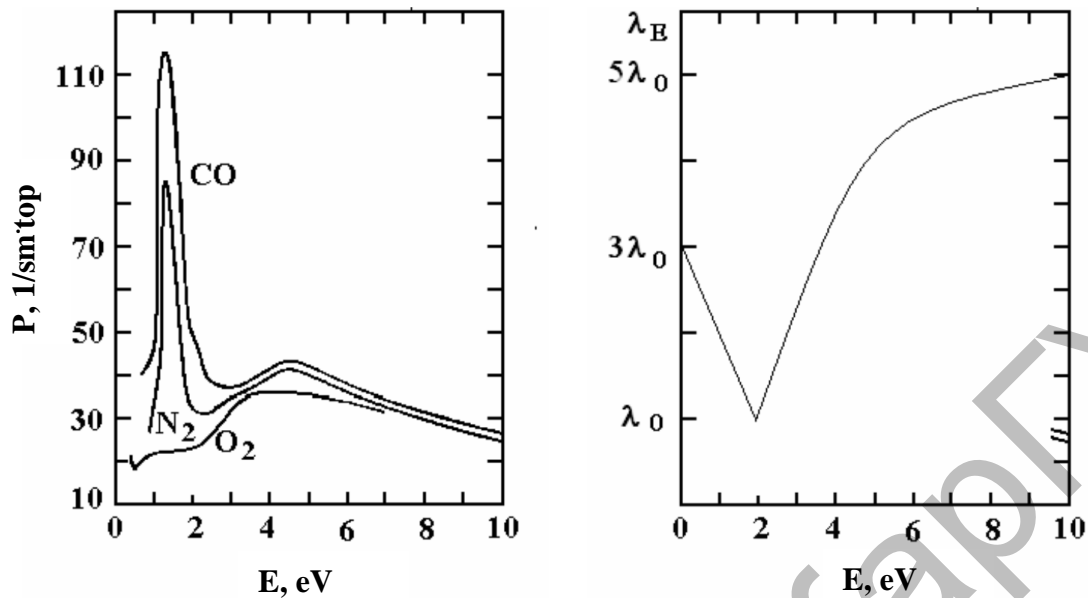


Fig. 1. Collision probability in O_2 , N_2 and CO (a) and free-path length approximation in N_2 (b)

For the purpose of statistic testing the free-path length shall be considered a random value distributed within the range $(0, \infty)$ with a probability density of

$$f(\lambda) = H e^{-H\lambda},$$

where H is the total interaction cross-section [3], wherefrom a formula of free-path length simulation can be derived:

$$\lambda = -\lambda_E \ln r. \quad (3)$$

Here and further on r is a specific value of a uniformly distributed number within the $[0, 1]$ interval obtained by means of statistic testing.

2. Elastic and inelastic collisions of electrons with gas molecules

Collisions of electrons with molecules can be elastic and inelastic events. Upon an elastic collision there happens a change in movement directions and in speed of colliding particles; the particles, impulses- and cinematic energy exchange takes place; however intrinsic energy of the particles remains unchanged. Upon an inelastic collision both intrinsic energy and molecule state change. Presented in Fig. 2 are experimental comparative relations of cross-sections of elastic- and inelastic (rotational-, vibrational- and electronic excitations) contacts of electrons and molecules N_2 [2]. Analysis of the figures proves that the ratio of the cross-sections of elastic and inelastic events within energy range from 0 to 0.1 eV is approximately 100:1 (rotational excitations), while within the energy range from 0.1 to 10 eV there happens a rise of inelastic events relative to elastic events up to approximately 2:1 ratio (total cross-section of rotational, vibrational and electronic excitations and ionization; with a further energy increase (>10 eVt) the latter ratio of 2:1 is retained. Similar relations for molecules H_2 are of the same qualitative nature.

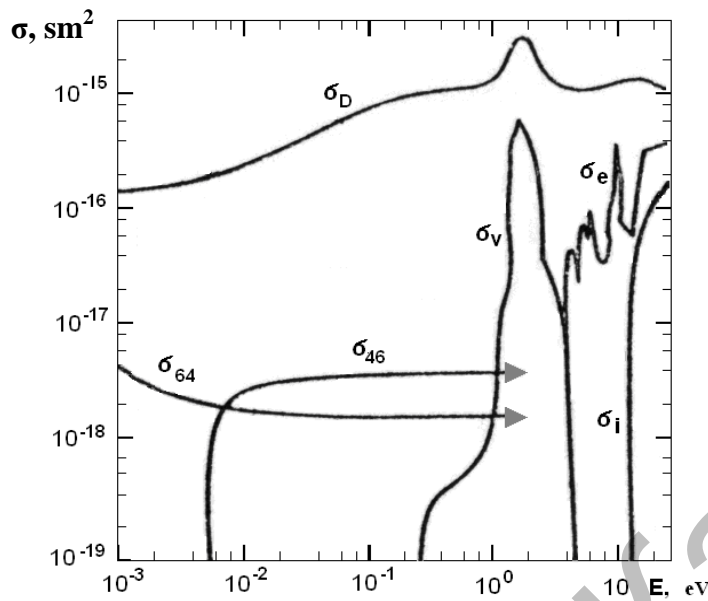


Fig. 2. Cross-sections comparison for various processes at electrons colliding molecules N_2 : σ_D – elastic transition event; σ_{46} and σ_{64} are rotational excitations from level $j=4$ to the level $j=6$ (theoretical); σ_v is total excitation of 8 vibrational levels; σ_e is total excitation of electronic levels with energies ranging from 5 to 14 eV; σ_i is ionization

Since collision cross-section is proportional to its probability, the values of above mentioned relations can be used to evaluate on a first approximation the probability of elastic and inelastic interactions at various sections of electron energy effective area in accordance with a diagram presented in Fig. 3.

Analytically the present diagram can be expressed as follows:

$$Collisions = \begin{cases} elastic, & 0 \leq r \leq P_e \\ inelastic, & P_e < r \leq 1, \end{cases} \quad (4)$$

where probability of elastic collision is

$$P_e = \begin{cases} 0.99, & 0 \leq E \leq 0.1, \\ 0.99 - \frac{0.32(E-0.1)}{9.9}, & 0.1 < E \leq 10, \\ 0.67, & E > 10. \end{cases}$$

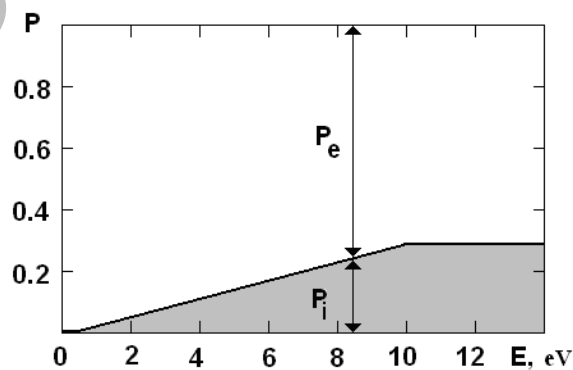


Fig. 3. Diagram of elastic and inelastic collisions simulations: P_e and P_i are probabilities of elastic and inelastic collisions

2.1. Elastic collisions

At elastic events electron scattering takes place without any energy losses at various angles. Presented in Fig. 4 are relations [2] of electron scattering cross-sections at atoms H_2 .

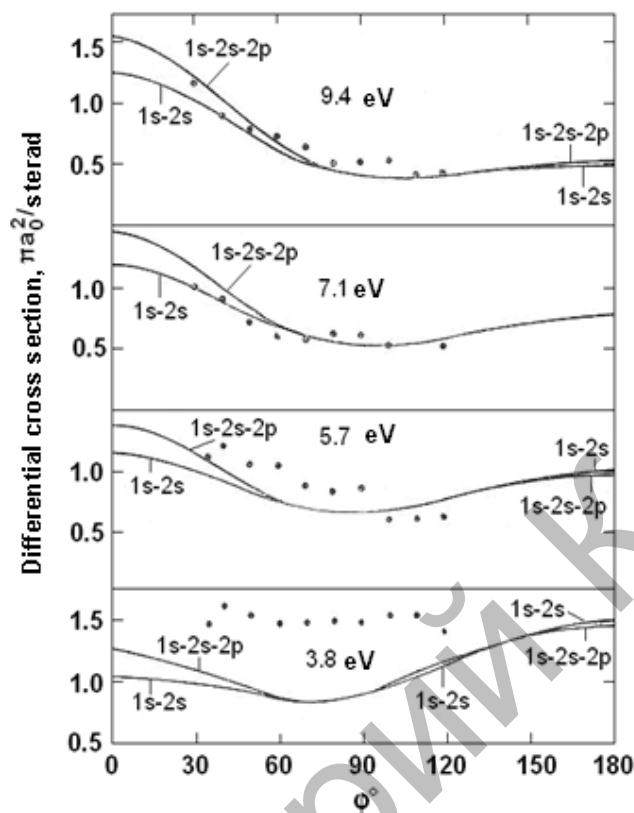


Fig. 4. Differential cross-section of electric elastic scattering on hydrogen atoms under four energy values of falling electrons. Points in the graph present experimental results, firm lines present results of quantum-mechanical calculations

The present plots allow to perform a piecewise-smooth patch of probability density $f(\varphi)$ of elastic scattering angles for the purpose of practical use (refer to Fig. 5).

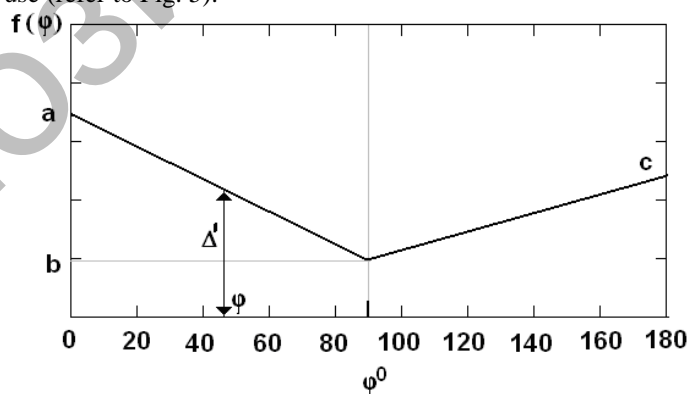


Fig. 5. Diagram of probability density of scattering angles

Therefore analytical expression for $f(\varphi)$ function will be as follows:

$$f(\varphi) = \Delta' = \begin{cases} a - \frac{a-b}{90}\varphi, 0 \leq \varphi \leq 90, \\ c - \frac{c-b}{90}(180 - \varphi), 90 < \varphi \leq 180. \end{cases} \quad (5)$$

Data presented in Fig. 4 allow to evaluate relative dependence of a and c parameters and energy E of an electron falling upon a molecule:

$$a(E)/b=E/3, c(E)/b=4-0.4E.$$

By means of algorithmic methods the scattering angles can be simulated like discrete quantities, e.g. quantities preset at an interval of 1° according to a standard pattern described below.

Parameter b is assumed to be equal to 1. Parameters a and c are calculated for each energy value. For each $\varphi_i=i, i=0..179$ angle the value Δ'_i is calculated in accordance with the expressions (5) (refer to Fig. 6). For high energy values in the area of $[90^\circ, 180^\circ]$ angles under $\Delta'_i < 0$ it shall be assumed that $\Delta'_i=0$. Assumptions made are in accordance with the known facts which prove the decrease of inverse scattering in proportion to the electron energy increase.

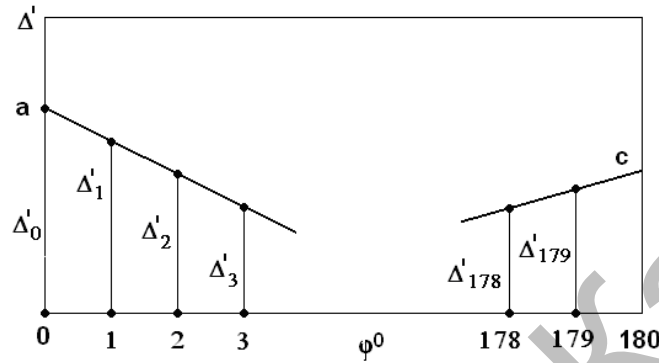


Fig. 6. Discrete distribution of scattering angle

Further normalized quantities (relative probabilities) $\Delta_i = \Delta'_i / \Delta'_Z$, где $\Delta'_Z = \sum_0^{179} \Delta'_i$, are calculated. Calculated are

coordinates of points $\xi_{i+1} = \sum_{i=0}^i \Delta_i, i=0..179$, while $\xi_0=0$. Please note that $\xi_{180}=1$.

Determination of scattering angle φ_i at each experiment is performed in accordance with $\xi_i \leq r < \xi_{i+1}, i=0..179$ condition (refer to Fig. 7). It appears that the probability of scattering at an angle of φ_i is proportional to the length of section Δ_i . Under assumption that scattering angle φ is uniformly distributed within the $[\varphi_i, \varphi_{i+1}] = 1^\circ$ range, its final value can be calculated as follows:

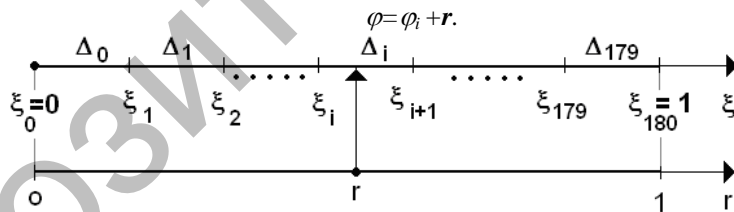


Fig. 7. Elastic scattering angles simulation

2.2. Inelastic collisions

Upon an inelastic collision an electron imparts a part of its energy and changes direction of its original movement.

SCATTERING ANGLES. It is well known that there is a small probability of inelastic scattering to large angles – except for the elements of small atomic number [2]. Experimental results obtained upon examination of relation between elastic and inelastic collisions (refer to Fig.8) - because of high complexity and low reliability of experimental methods used for this purpose - can bring us to the only conclusion that there are common trends in the processes under study, and more particular, to a conclusion of practical coincidence of angular distribution of electrons under elastic and inelastic interactions of electrons and molecules.

Quantitative assessments based on the data cited above can hardly be used for practical purposes. All the aforesaid proves that the above suggested methods of simulation of electron scattering angle at elastic collision based on quantum-mechanical representations can be also applicable to inelastic interactions.

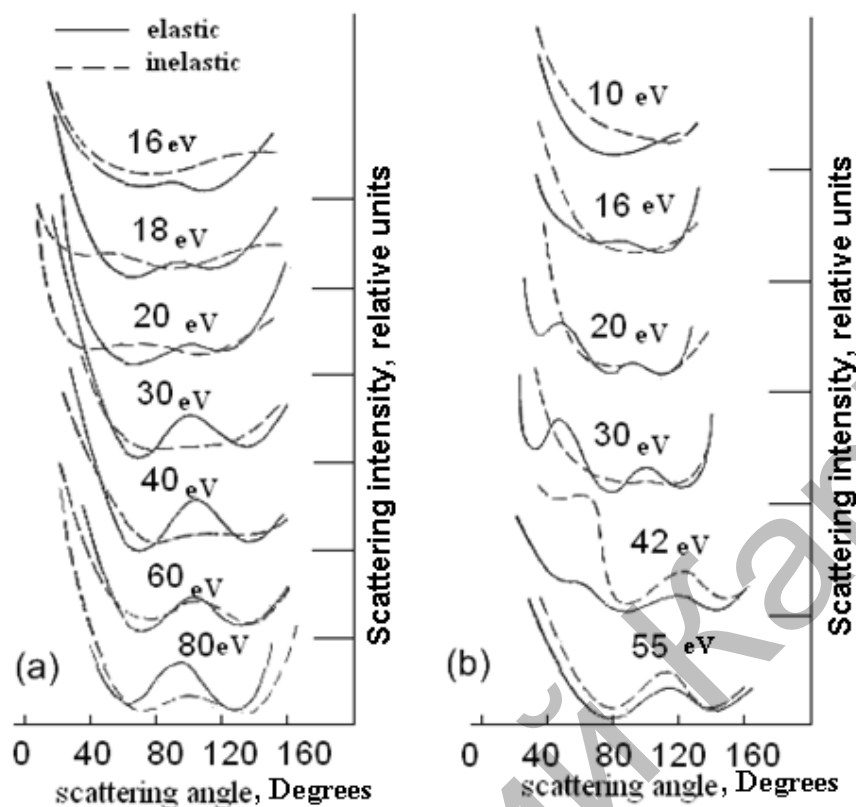


Fig. 8. Experimentally measures angular distribution of electrons of various energies scattered by argon (a) and mercury (b) atoms

ENERGY LOSSES. Since an electron at an inelastic interaction with a molecule can transfer a part of its energy to the molecule thus initializing rotational transition (up to tenths of eV), vibrational-rotational transition (from tenths of eV to several eV units), electron-vibrational-rotational transitions (above several eV units) and ionization (above 10 eV), it is quite reasonable to assume as equally probable any loss of any part of initial electron energy under such an interaction, or in formalized representation

$$E_i = E - rE = E(1-r) = Er, \quad (6)$$

where E_i is electron energy upon an inelastic interaction.

2.3. Determination of component values of electron speed after interaction

Direction cosines determining changed direction of electron movement after scattering under preset electron speed components v_x , v_y and v_z which determine actual direction of electron speed and a given of scattering angle φ (at elastic and inelastic interactions) can be calculated by means of analytic geometry methods. Presented in Fig. 9 is correlation between initial (\vec{n}) and final (\vec{n}_1) directions of movement required to derive working formulae.

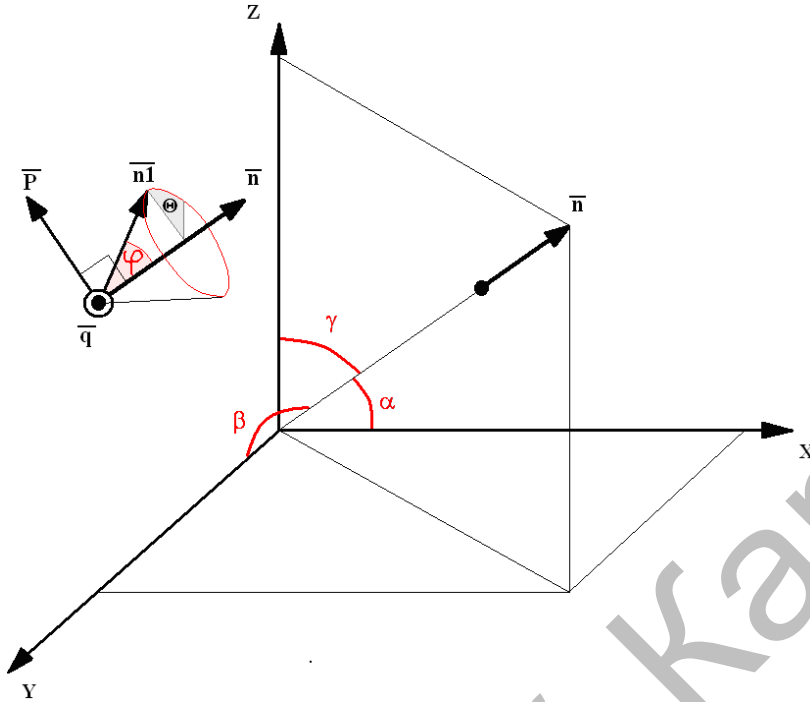


Fig. 9. On determination of new values of direction cosines of electron speed at a given scattering angle ϕ

Introduced here is an orthogonal basis of vectors $\vec{n}, \vec{q}, \vec{p}$ where the vector \vec{n} is codirectional with the electron speed $\vec{v} = v_x \vec{i} + v_y \vec{j} + v_z \vec{k}$ before collision, and directional cosines of initial speed vector $\cos \alpha = \frac{v_x}{v}$,

$$\cos \beta = \frac{v_y}{v}, \quad \cos \gamma = \frac{v_z}{v} \quad \text{where speed module is } v = \sqrt{v_x^2 + v_y^2 + v_z^2}.$$

Determined next is parameter $\text{mincos} = \min[|\cos(\alpha)|, |\cos(\beta)|, |\cos(\gamma)|]$.

Let us assume $\text{mincos} = |\cos(\alpha)|$ - then vector \vec{p} components can be obtained as follows:

$$p_x = 0, \quad p_y = \frac{\cos \gamma}{\sqrt{\cos^2 \gamma + \cos^2 \beta}}, \quad p_z = \frac{\cos \beta}{\sqrt{\cos^2 \gamma + \cos^2 \beta}},$$

If $\text{mincos} = |\cos(\beta)|$, then

$$p_x = \frac{\cos \alpha}{\sqrt{\cos^2 \alpha + \cos^2 \gamma}}, \quad p_y = 0, \quad p_z = \frac{\cos \beta}{\sqrt{\cos^2 \alpha + \cos^2 \gamma}},$$

Assume $\text{mincos} = |\cos(\gamma)|$, then

$$p_x = \frac{\cos \beta}{\sqrt{\cos^2 \alpha + \cos^2 \beta}}, \quad p_y = \frac{\cos \alpha}{\sqrt{\cos^2 \alpha + \cos^2 \beta}}, \quad p_z = 0.$$

Now vector \vec{q} component can be calculated by means of respective sequence of formulae. First absolute values of components are determined:

$$q_{0x} = p_z \cos \beta - p_y \cos \gamma,$$

$$q_{0y} = p_x \cos \gamma - p_z \cos \beta,$$

$$q_{0z} = p_y \cos \alpha - p_x \cos \beta.$$

Next normalized values are determined

$$q_x = \frac{q_{0x}}{q}, \quad q_y = \frac{q_{0y}}{q}, \quad q_z = \frac{q_{0z}}{q},$$

where the vector length $q = \sqrt{q_{0x}^2 + q_{0y}^2 + q_{0z}^2}$.

Angle Θ determining the orientation of electron speed vector directed upon collision along \vec{n}_1 (refer to Fig. 9) is simulated as a uniformly distributed angle within a range of $[0, 2\pi]$, which means:

$$\Theta = r2\pi.$$

Then new directional cosines (after scattering at angle φ) can be determined by means of the following formulae sequence:

$$\begin{aligned} \cos\alpha_0 &= \cos\alpha \cos\varphi + \sin\varphi [p_x \cos\Theta + q_x \sin\Theta], \\ \cos\beta_0 &= \cos\beta \cos\varphi + \sin\varphi [p_y \cos\Theta + q_y \sin\Theta], \\ \cos\gamma_0 &= \cos\gamma \cos\varphi + \sin\varphi [p_z \cos\Theta + q_z \sin\Theta], \\ \cos\alpha &= \frac{\cos\alpha_0}{s}, \cos\beta = \frac{\cos\beta_0}{s}, \cos\gamma = \frac{\cos\gamma_0}{s}, \end{aligned}$$

$$\text{where } s = \sqrt{\cos^2\alpha_0 + \cos^2\beta_0 + \cos^2\gamma_0}.$$

As a result the electron speed components after interaction with a molecule can be calculated with the help of the following formulae:

$$v_x = \sqrt{\frac{2E}{m}} \cos\alpha_0, v_y = \sqrt{\frac{2E}{m}} \cos\beta_0, v_z = \sqrt{\frac{2E}{m}} \cos\gamma_0, \quad (7)$$

where E is electron energy after collision; the energy value is retained upon an elastic collision and reduced ($E=E_i$) upon an inelastic collision (refer to Section 2.2), m – electron mass.

3. Algorithm and results of electron movement simulation under conditions of collisions with gas molecules

To perform calculations of electron movement under conditions of interactions with gas molecules, the following values have been set: gas pressure (P) and temperature (T) and also gas-kinetic diameter of a molecule. On the basis of correlation (1) the free path length (λ_0) in gas-kinetic approximation is determined and trajectory simulation is initiated.

Simulation of each trajectory section starts with determination of electron free path length according to actual value of its kinetic energy (E) (refer to formula (2)) and statistic simulation of some particular free path length under given experiment (3). In the course of calculation with an excess of trajectory length l in the free path length section under study λ , the time of integration step dT is decreased proportionally up to dT_{last} at the last integration interval; then integration with a obtained step dT_{last} is performed (refer to Fig. 10), whereupon a collision of electron with a molecule is assumed to happen.

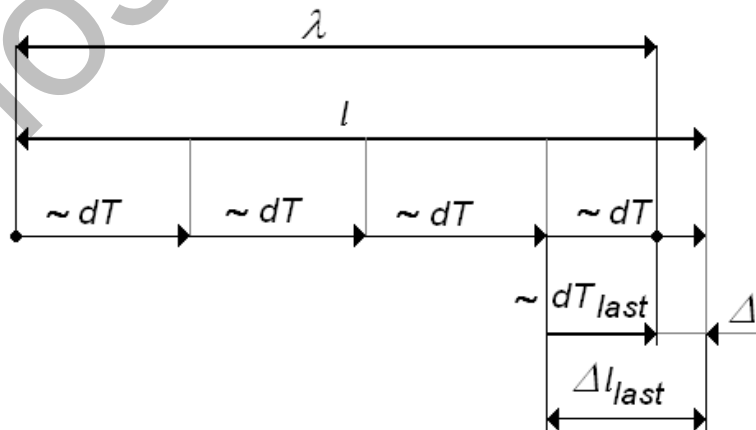


Fig. 10. Determination of the last integration step before collision: $dT_{last} = dT \frac{\Delta l_{last} - \Delta}{\Delta l_{last}}$, where $\Delta = l - \lambda$.

Then according to condition (4) the nature of collision – elastic or inelastic - can be determined.

For elastic collisions the scattering angle φ can be determined according to the diagram presented in Section 2.1 and electron speed components after interaction with a molecule can be determined by means of resulting formula (7) of Section 2.3.

For inelastic collisions the scattering angle φ , energy (6) and electron speed components (7) after interaction with a molecule can be determined according to the diagram presented in Section 2.1.

Then the same calculation process is applied to the next trajectory segment.

Algorithm described above constitutes a basis of a software module intended to simulate a path of current flow under conditions of electrons interaction with gas molecules.

The software module is integrated into FOCUS [4] software application designed for numerical investigation of electron optic systems.

Adequacy check of the above model was performed on an experimental mockup consisting of a vacuum diode with planar cathode and anode. Research proves that upon letting-to-air, initial current (vacuum current) was approximately four-times reduced. Calculations performed in accordance with the described methods yield the same relative order of decrease of emitted electrons when moving towards the anode.

Presented in Fig. 11 are the results of trajectory analysis of a DC arc melting furnace under atmospheric pressure and with an external magnetic field with an induction of 1mT and 10mT imposed transversely to the symmetry axis of the system. At an induction value in 50 mT order of magnitude (not presented in the drawing) the arc slants to the furnace body (which would result in discharge stripping).

The above analysis yields a conclusion that induction value of $B=10$ mT is critical for unfavorable arc slanting. Operational experience with DC arc melting furnaces [5] reveals some premature wearing spots in the isolation lining. Measurement of induction value of magnetic field generated by a system of feed conductors gave a result in 10 mT order of magnitude. The magnetic field direction was in coincidence with the field direction which resulted in arm slanting towards damaged spot (due to local overheating) in the isolation lining.

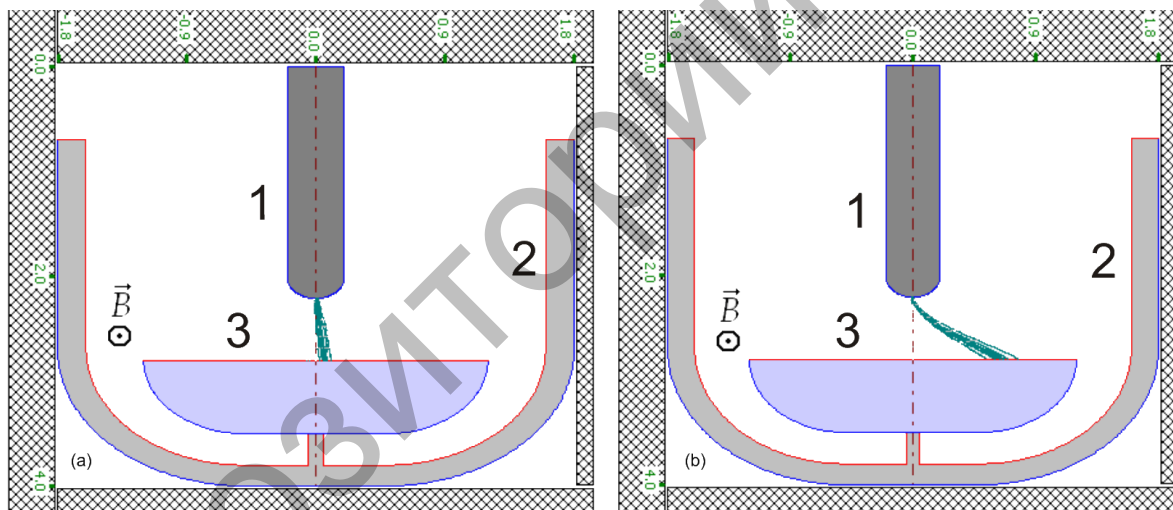


Fig. 11. Path of electrons emitted from an anode spot under condition of collisions with ambient air molecules and under imposition of an external magnetic field: (a) $B=1$ mT, (b) $B=10$ mT. Presented here: 1 – cathode, 2 – furnace body, 3 – metal bath

Conclusion

Numerical model of electron movement inside gas media was developed. Respective software module integrated into FOCUS [4] software application designed for numerical investigation of electron optic systems was obtained. Experimental test of the developed model was performed.

References:

1. Yavorsky B.M., Detlaf A.A. Physics Reference Book for Engineers and University Students. Moscow : Nauka Publishers, 1971. p. 940
2. Y.P. Raiser. Physics of Gas Discharge. Study Guide.- Moscow: Nauka Publishers, p.1987.- 592 .
3. Sobol I.M.. Monte Carlo numerical methods. Moscow: Nauka Publishers, p. 1973. 312.

4. Trubitsyn A.A. FOCUS software application designed for simulation of axially symmetric electron optics systems: algorithms and characteristics // Applied Physics. No.2. 2008, p. 56-62.
5. Bogdanovsky A.S. Experience of DC furnace DPPTU-20 operation in a steel foundry at OAO Tyazhpresmash // Metallurgy in Machine-building industry. No.1, 2007, p. 18-24.

Репозиторий КарГУ